NANO LETTERS

2006
Vol. 6, No. 12
2949−2954

Template-Assisted Formation of Gradient Concentric Gold Rings

Suck Won Hong, Jun Xu, and Zhiqun Lin*

Department of Materials Science and Engineering, Iowa State University, Ames, Iowa 50011

Received October 12, 2006; Revised Manuscript Received November 1, 2006

ABSTRACT

Gradient concentric rings of polymers, including (poly[2-methoxy-5-(2-ethylhexyloxy)-1,4-phenylenevinylene] (MEH-PPV) and poly(methyl methacrylate) (PMMA), with unprecedented regularity were formed by repeated "stick-slip" motion of the contact line in a sphere-on-flat geometry. Subsequently, polymer rings served as templates to direct the formation of concentric Au rings. Three methods were described. The first two methods made use of either UV (i.e., on MEH-PPV) or thermal treatment (i.e., on PMMA) on Au-sputtered polymer rings, followed by ultrasonication. The last method, however, was much more simple and robust, involving selective removal of Au and polymer (i.e., PMMA) consecutively.

Introduction. Two-dimensional (2D) periodic structures are attractive for a wide range of applications in optics,[1,2] optoelectronics,[3,4] photonics,[5] electronics,[6] magnetic materials,[7] and biotechnology.[8] A variety of self-assembled systems have been utilized as templates to produce well-ordered 2D structures with no need of lithography, including microphase-separated block copolymers,[7,9] hexagonally ordered arrays (i.e., breath figures) made by the condensation of micron-size water droplets on the surface of a polymer solution,[10] self-assembly of colloidal crystals,[11] and self-organized mesoporous silica.[12]

Dynamic self-assembly of dispersions through irreversible solvent evaporation of a drop from a solid substrate is widely recognized as a nonlithography route for one-step creation of complex, large-scale structures.[13−15] The flow instabilities within the evaporating droplet, however, often result in nonequilibrium and irregular dissipative structures,[16] e.g., convection patterns, fingering instabilities, and so on. Therefore, to fully utilize evaporation as a simple tool for achieving well-ordered 2D structures, it requires delicate control over flow instabilities and evaporation process. Recently, self-organized gradient concentric ring patterns have been produced by constraining a drop of polymer solution in a restricted geometry composed of either two cylindrical mica surfaces placed at a right angle to one another or a sphere on a flat surface (i.e., *two* surfaces).[17−19] The unprecedented regularity makes these polymer rings intriguing templates for producing concentric metal rings. Here, we report on fabrications of gradient concentric gold (Au) rings with nanometers in height and microns in width, replicated from templates of polymer rings. The gradient concentric polymer rings[17−19] were formed on Si- or Au-coated ITO substrate via drying mediated self-assembly from a capillary-held polymer solution in the sphere-on-flat geometry (Figure 1a). Two polymers were employed as nonvolatile solutes: (poly[2-methoxy-5-(2-ethylhexyloxy)-1,4-phenylenevinylene] (MEH-PPV) and poly(methyl methacrylate) (PMMA). Subsequently, polymer rings served as templates for making Au rings by several methods, as schematically illustrated in Figure 2.

Experimental Section. *Evaporation-Induced Self-Assembly of Polymer Rings in a Sphere-on-Flat Geometry.* Si substrates and spherical lenses made from fused silica (radius of curvature ∼1 cm) were cleaned with a mixture of sulfuric acid and Nochromix. The indium tin oxide (ITO) glasses were cleaned with acetone, DI water, and filtered ethanol and then blow-dried with N_2. A sphere-on-flat geometry inside a chamber was constructed and implemented as follows. Both spherical lens and Si (or ITO) were firmly fixed at the top and the bottom of sample holders in the chamber, respectively. An inchworm motor was used to bring the upper sphere into contact with the lower stationary Si (or ITO) substrate. Before they contacted (i.e., separated by a few hundred micrometers), 25 μL of polymer toluene solution was loaded and trapped between the sphere and Si (or ITO) due to the capillary force. The sphere was finally brought into contact with Si (or ITO) substrate by the inchworm motor such that a capillary-held polymer solution formed with evaporation rate highest at the extremity, as schematically illustrated in Figure 1a. This led to controlled, repetitive "stick-slip" motion of the three-phase contact line, which moved toward the center of the sphere/Si contact (i.e., contact center in Figure 1b) during the course

* Corresponding author. Email: zqlin@iastate.edu.

10.1021/nl0624061 CCC: $33.50
Published on Web 11/16/2006

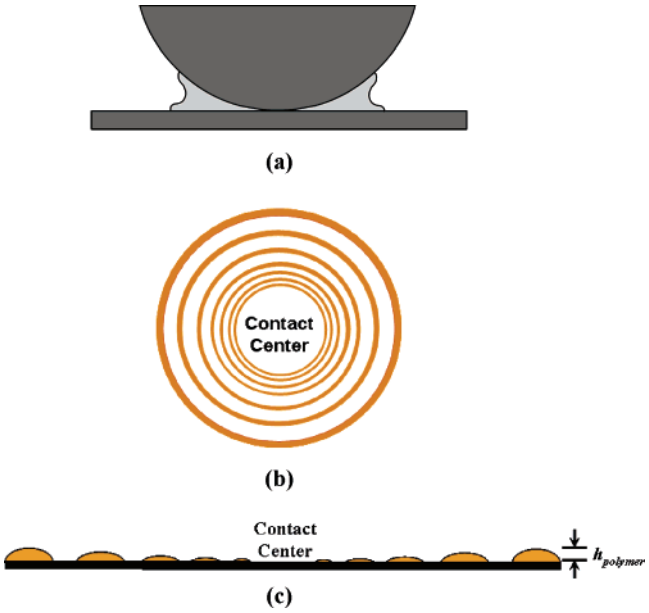

Figure 1. Schematic illustrations of (a) a drop of polymer solution placed in a sphere-on-flat geometry, (b) gradient concentric polymer rings produced by solvent evaporation in the geometry shown in (a), and (c) side view of polymer rings formed in (b), exhibiting a gradient in the center-to-center distance between adjacent rings, λ_{C-C}, and the height of the ring, $h_{polymer}$, from leftmost across the "contact center" to rightmost. The sphere/Si (or ITO) contact area is marked as "contact center".

of solvent evaporation. As a result, gradient concentric polymer rings were formed. Two polymers were used as nonvolatile solutes to produce gradient concentric rings: a linear conjugated polymer, poly[2-methoxy-5-(2-ethylhexyloxy)-1,4-phenylenevinylene] (MEH-PPV) (molecular weight, MW = 50−300 kg/mol) and poly(methyl methacrylate) (PMMA) (number average MW, M_n = 534 kg/mol and polydispersity, PDI = 1.57). The concentration of MEH-PPV toluene solution was 0.05 mg/mL. For PMMA, the concentrations of the solutions were 0.5 mg/mL and 0.125 mg/mL, used in methods B and C, respectively. Only the ring patterns on Si or ITO substrates were utilized as templates.

Template-Assisted Formation of Concentric Au Rings. Method A: Use of MEH-PPV Rings on Si as Templates. Gold (Au), 16 nm thick, was sputtered on MEH-PPV rings on Si substrate (Figure 2a). The sample was then exposed to UV radiation (Mineralight lamp model UVGL-25; λ = 254 nm) for 15 h to degrade MEH-PPV buried underneath Au. Afterward, the sample was ultrasonicated in toluene for 10 min to remove degraded MEH-PPV. A Au replica was thus obtained (Figure 3). Finally, the Au replica was cleaned up with sulfuric acid.

Method B: Use of PMMA Rings on Si as Templates. Similar to method A, 36 nm thick Au was sputtered on PMMA rings on Si substrate (Figure 2b). To achieve Au rings, the sample was then placed in a furnace at 400 °C for 2 h to thermally decompose buried PMMA, followed by extensive ultrasonication in toluene for 15 min.

Method C: Use of PMMA Rings on Au-Coated ITO Glass as Templates. In this method, 36 nm thick Au was first

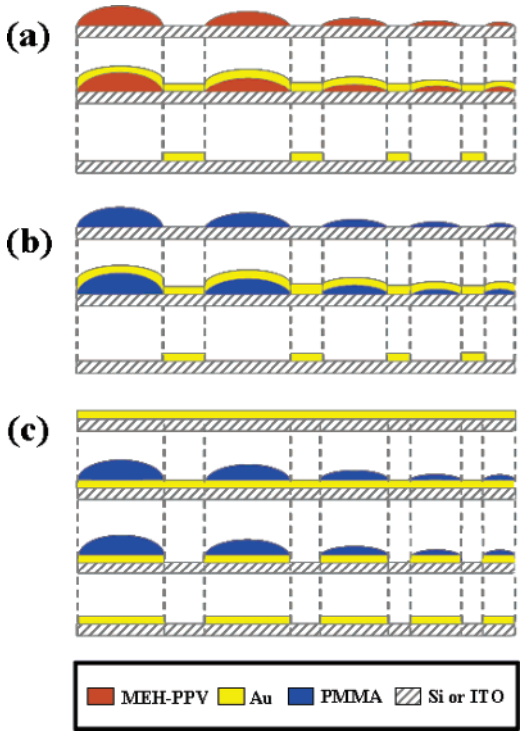

Figure 2. Schematic stepwise representation of formation of gradient concentric Au rings. (a) Evaporation-induced self-assembly of MEH-PPV rings on Si substrate from MEH-PPV toluene solution, showing a decrease in λ_{C-C} and h from outermost ring (left) toward the "contact center" (right). Then a layer of Au was thermally evaporated, followed by UV degradation of MEH-PPV and final removal by ultrasonication. (b) Gradient concentric PMMA rings formed in the same way as illustrated in (a). Subsequently, a layer of Au was deposited, followed by pyrolysis of PMMA and final removal by ultrasonication. (c) A layer of Au was deposited on ITO substrate. Then PMMA rings were formed. Afterward, Au between PMMA rings was selectively removed with the KI/I_2 DI water solution. Finally, concentric Au rings were achieved by washing off PMMA on their top with acetone.

thermally deposited on ITO glass. To ensure good adhesion between Au and ITO, 2 nm thick TiO_2 was evaporated on ITO glass. PMMA rings were then formed on Au-coated ITO substrate. Afterward, Au between PMMA rings were selectively removed with a mixture of potassium iodide/iodide DI water solution (KI/I_2/DI water = 5 g/1.25 g/50 mL) for Au for 1 min. Finally, PMMA rings were completely rinsed off with acetone, thereby exposing Au underneath.

Characterization. An Olympus BX51 optical microscope (OM) in the reflection mode was used to investigate the patterns deposited on Si or ITO substrates. Atomic force microscopy (AFM) images on patterns on Si (or ITO) surface were obtained using a Digital instruments Dimension 3100 scanning force microscope in the tapping mode. BS-tap300 tips from Budget Sensors with spring constants ranging from 20 to 75 N/m were used as scanning probes. The scanning electron microscopy (SEM) studies were performed on a JEOL 6060LV SEM, operating at 5 kV accelerating voltage.

Results and Discussion. A drop of MEH-PPV or PMMA toluene solution bridged the gap between a spherical lens and a Si (or ITO) substrate, forming a capillary-held solution (Figure 1a) (see Experimental Section).[17−19] The evaporation

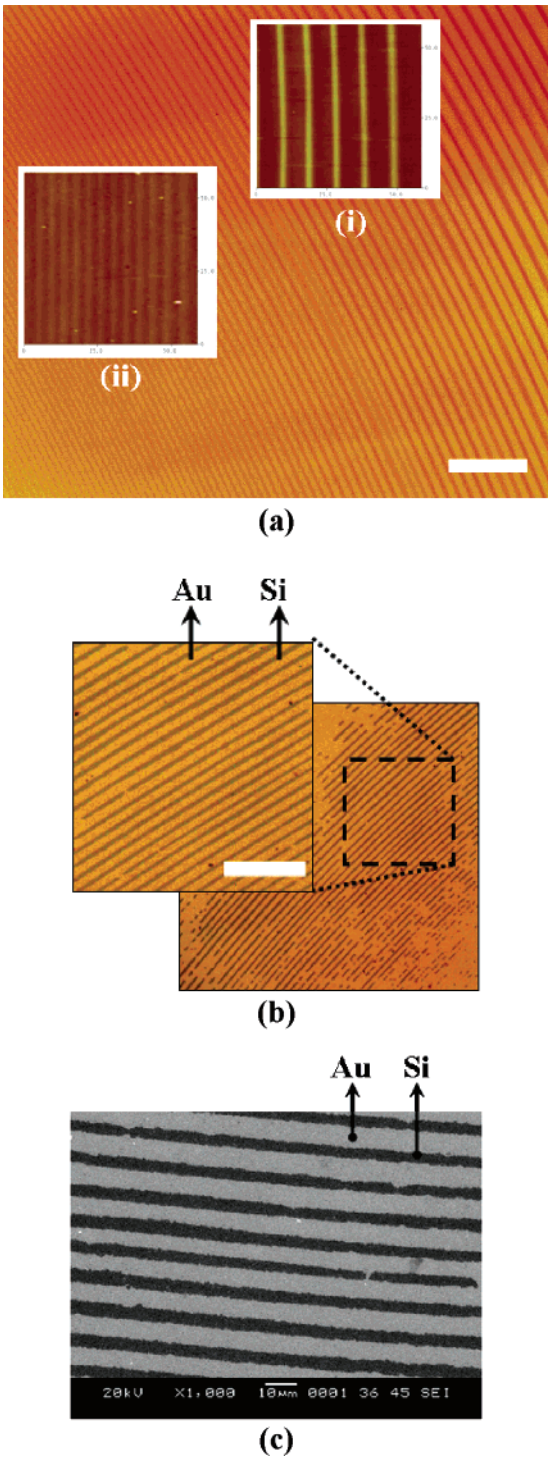

Figure 3. (a) Optical micrograph of gradient concentric MEH-PPV rings formed via controlled, repetitive "stick-slip" motion of the contact line in the sphere-on-flat geometry (Figure 1a). The scale bar is 200 μm. Two representative 2D AFM height images are shown as insets, demonstrating a decrease in λ_{C-C} and h with increasing proximity to the center of sphere/Si contact (i.e., from location (i) to (ii)). The AFM image size is 60 $\times$ 60 μm^2. The z scale is 50 nm. (b) Optical micrograph of Au rings after ultrasonicating off degraded MEH-PPV in which MEH-PPV was not completely removed. A close up is shown in the upper left. The dark and yellow stripes are Si rings and Au rings, respectively. The scale bar is 70 μm. (c) SEM image of Au rings. The dark and gray stripes correspond to Si rings and Au rings, respectively.

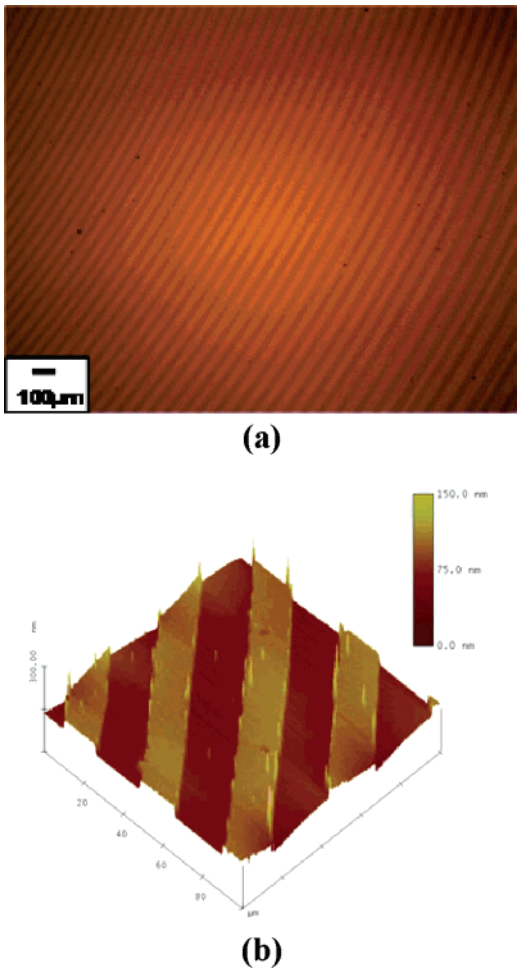

Figure 4. (a) Optical micrograph of gradient concentric Au rings on Si substrate fabricated using method B (i.e., schematic b in Figure 2). The scale is 100 μm. (b) A representative 3D AFM height image of Au rings. The image size is 100 $\times$ 100 μm^2. The z scale is 150 nm.

was restricted at the capillary edges.[17−19] Evaporative loss of toluene at the capillary edges caused the pinning of the contact line (i.e., "stick"), thereby forming the outmost polymer ring. As solvent evaporated, the initial contact angle of the capillary edge decreased gradually to a critical angle at which the capillary force (depinning force) became larger than the pinning force,[19] leading the contact line to hop to a new position (i.e., "slip") so that a new ring deposited. Repetition of the "stick-slip" motion of the contact line resulted in the formation of concentric rings of the polymer toward the center of sphere/Si (or ITO) contact (i.e., contact center in Figure 1b). The patterns chronicled the moments of arrested contact line motion in the capillary bridge. The center-to-center distance, λ_{C-C}, between polymer rings and height of the ring, h, were found to decrease with increasing proximity to the contact center (Figure 1c) as a result of the competition of linear pinning force and nonlinear capillary force.[19] It is noteworthy that the restricted geometry (i.e., sphere-on-flat) carries the advantage over cases in which a droplet is allowed to evaporate on a single surface,[13−15] namely providing a unique environment for controlling the

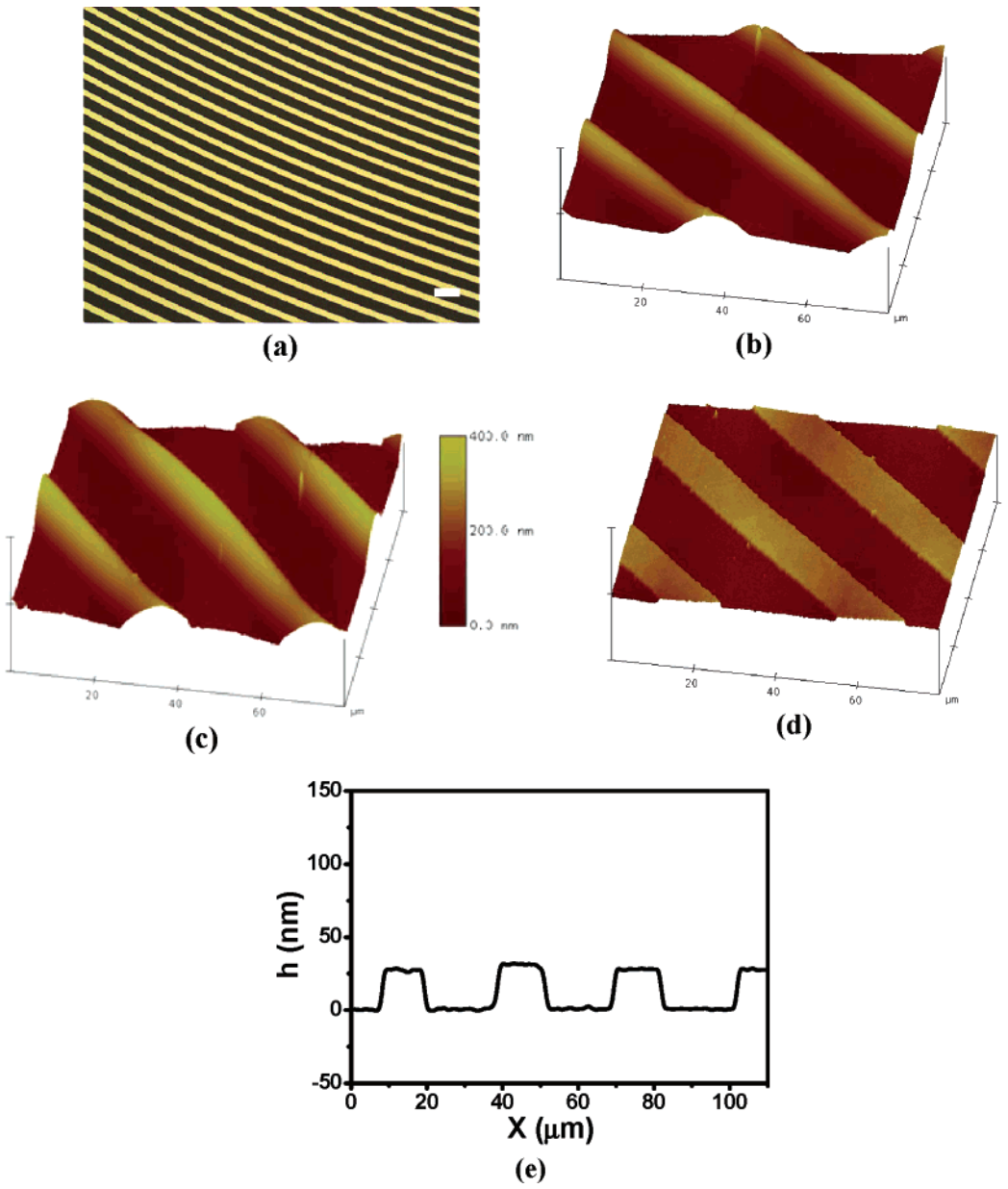

Figure 5. (a) Optical micrograph of concentric Au rings on ITO surface. The scale bar is 50 μm. (b−d) Representative 3D AFM height images (80 × 80 μm^2), corresponding to the stages illustrated in Figure 2c. The *z* scale is 400 nm. (b) PMMA rings on Au-coated ITO substrate. (c) PMMA rings after removal of Au between the rings with the KI/I_2 DI water solution. (d) Au rings obtained after rinsing with acetone to eliminate PMMA. (e) Typical cross-section of Au rings in (d).

flow within an evaporating droplet, which in turn regulates the structure formation with excellent reproducibility.

Subsequently, the polymer ring patterns served as templates for producing Au rings using three methods as depicted in Figure 2. Method A utilized MEH-PPV rings formed by evaporation-induced self-assembly from MEH-PPV toluene solution confined in the sphere-on-flat geometry (Figure 2a). Gradient concentric rings are clearly evident (Figure 3a). The λ_{C-C} and h were observed to decrease as the evaporation front moved toward the sphere/Si contact center (i.e., from upper right to lower left). The section analysis of two representative 2D AFM height images (insets in the optical micrograph) yields $\lambda_{C-C} = 9.6$ μm and $h = 7.6$ nm at location (i) and $\lambda_{C-C} = 4.3$ μm and $h = 1.3$ nm at location (ii). It is of interest to note that the width of MEH-PPV rings is much smaller than the space between the rings. After sputtering a layer of 16 nm Au on the surface of MEH-PPV rings, the sample was subjected to UV irradiation (see Experimental Section). Finally, MEH-PPV rings together with Au covering on their top were removed by ultrasonication, leaving behind Au rings that were originally deposited between MEH-PPV rings. Incomplete removal of buried MEH-PPV was observed as shown in Figure 3b, which was most likely due to very low power of UV source used so that MEH-PPV was not readily photodegraded completely. Locally, Au rings appeared as the stripes (SEM image in Figure 3c). The width of Au stripes is much wider than that of Si stripes (a close-up view of optical micrograph in Figure 3b and c), which correlates well with the optical microscopy observation before the deposition of Au (Figure 3a). The energy

dispersive X-ray analysis (EDX) on the Au replica revealed that no Au signal were detected in the region between original MEH-PPV rings, indicating that MEH-PPV rings together with Au on the top were completely detached from Si substrate.

In method B (Figure 2b), gradient concentric PMMA rings produced by controlled, repetitive "stick-slip" motion in the restricted geometry consisting of a spherical lens and a Si substrate were utilized as templates. A 36 nm Au was sputtered. Instead of applying UV radiation to degrade PMMA due to rather low UV power, PMMA rings buried under Au were thermally decomposed at 400 °C. The Au ring replica was obtained eventually after ultrasonication in toluene (optical micrograph; Figure 4a). The order of Au rings was reminiscent of the arrangement of PMMA rings and was not affected by the thermal treatment and subsequent ultrasonication. A typical 3D AFM height image of Au replica is shown in Figure 4b. The λ_{C-C} and h are 30 μm and 36 nm, respectively. It should be noted that complete removal of pyrolyzed PMMA was achieved by sonication as compared to the case in MEH-PPV (Figure 3b); however, prolonged sonication was found to cause Au rings to delaminate from the Si substrate.

Rather than performing the sputtering of Au on polymer ring patterns to achieve Au rings as demonstrated in methods A and B (Figures 3 and 4), a much more simple method (method C) was to first thermally evaporate a thick layer of Au on ITO, followed by the formation of concentric polymer rings and successive removal of Au (between the polymer rings) and polymer on the top of buried Au.[20] As depicted in Figure 2c, PMMA rings were formed at the surface of Au-coated ITO. The sample was then treated with the KI/I_2 DI water solution to selectively dissolve Au between PMMA rings. Finally, the sample was rinsed with acetone thoroughly to remove PMMA, thereby exposing underlying Au as shown in Figure 5a. The 3D AFM height images corresponding to the steps illustrated in Figure 2c are shown in Figure 5b−d. The PMMA rings were humplike with the height, h, the width, w, and the center-to-center distance between PMMA rings, λ_{C-C}, are 114 nm, 14 μm, and 31 μm, respectively as determined by the AFM (Figure 5b). After the treatment with the KI/I_2 aqueous solution, h increased to 150 nm, while w and λ_{C-C} were unchanged (Figure 5c). The height of Au underneath PMMA rings was thus found to be 36 nm, which agreed well with the value obtained after removal of PMMA (Figure 5d). Rather than humplike rings (Figure 5b and c), stepwise rings were obtained, as are evidenced in Figure 5d and e. Slightly lower values of w (13.5 μm) and λ_{C-C} (30 μm) were obtained due to the fact that the AFM image was taken at the location that was slightly closer to the center of sphere/ITO contact. Compared to methods A and B in which extensive UV degradation (method A), high-temperature treatment (method B), and ultrasonication were applied (methods A and B), this method is much more simple, fast, and robust.

In conclusion, gradient concentric rings of polymers with unprecedented regularity were formed by repeated "stick-slip" motion of the contact line in a sphere-on-flat geometry. There is no restriction on polymer materials that can be used for forming highly ordered concentric rings and on substrates where polymer rings deposited. Subsequently, polymer rings served as templates to direct the formation of concentric Au rings. Three methods were described. The first two methods made use of either UV (i.e., on MEH-PPV) or thermal treatment (i.e., on PMMA) on Au-sputtered polymer rings, followed by ultrasonication. The last method, however, was much more simple and robust, involving selective removal of Au and polymer consecutively. The resulting metal rings organized in a concentric mode may offer possibilities for many applications, including annular Bragg resonators for advanced optical communications systems. It has been demonstrated that λ_{C-C} and h decrease nonlinearly with increasing polymer concentration.[19] Studies in order to dynamically tune the formation of gradient concentric rings of polymers by proper choice of the solvent, the interaction between the polymer and the substrate, and the curvature of the sphere, which in turn regulate the dimension of Au rings, are currently underway. The methods described should readily extend to the fabrication of gradient concentric rings of other metals and metal oxides (e.g., zinc oxide) for biomedical applications with little toxicity.[21] We envision that metal and/or metal oxide microstructures other than concentric rings, for example, spoke patterns, can be easily obtained from corresponding polymer templates produced in the sphere-on-flat geometry. Gradient concentric metal and/or metal oxide rings can serve as etching barriers for transferring patterns into Si substrate by reaction ion etching with SF_6 gas. A detailed study using organized metal and/or metal oxide rings as well as the abovementioned pattern-transferred Si as channels for microfluidic devices is currently underway.

Acknowledgment. This work was supported by the 3M Nontenured Faculty Award, the American Chemical Society Petroleum Research Fund (grant no. 42825-G7), and the University Research Grant (URG) at Iowa State University.

References

(1) Yabu, H.; Shimomura, M. *Langmuir* **2005**, *21*, 1709.
(2) Yabu, H.; Shimomura, M. *Adv. Funct. Mater.* **2005**, *15*, 575.
(3) Erdogan, B.; Song, L.; Wilson, J. N.; Park, J. O.; Srinivasarao, M.; Bunz, U. H. F. *J. Am. Chem. Soc.* **2004**, *126*, 3678.
(4) Song, L.; Bly, R. K.; Wilson, J. N.; Bakbak, S.; Park, J. O.; Srinivasarao, M.; Bunz, U. H. F. *Adv. Mater.* **2004**, *16*, 115.
(5) Joannopoulos, J. D.; Meade, R. D.; Winn, J. N. *Photonic Crystals: Modeling the Flow of Light*; Princeton University Press: Princeton, NJ, 1995.
(6) Jacobs, H. O.; Whitesides, G. M. *Science* **2001**, *291*, 1763.
(7) Thurn-Albrecht, T.; Schotter, J.; Kastle, C. A.; Emley, N.; Shibauchi, T.; Krusin-Elbaum, L.; Guarini, K.; Black, C. T.; Tuominen, M. T.; Russell, T. P. *Science* **2000**, *290*, 2126.
(8) Ostuni, E.; Chen, C. S.; Ingber, D.; Whitesides, G. M. *Langmuir* **2001**, *17*, 2828.
(9) Misner, M. J.; Skaff, H.; Emrick, T.; Russell, T. P. *Adv. Mater.* **2003**, *15*, 221.
(10) Bunz, U. H. F. *Adv. Mater.* **2006**, *18*, 973.
(11) Holland, B. T.; Stein, A. *Science* **1998**, *281*, 538.
(12) Lin, V. S.-Y.; Motesharei, K.; Dancil, K. S.; Sailor, M. J.; Ghadiri, M. R. *Science* **1997**, *278*, 840.
(13) Deegan, R. D.; Bakajin, O.; Dupont, T. F.; Huber, G.; Nagel, S. R.; Witten, T. A. *Nature* **1997**, *389*, 827.

(14) Deegan, R. D. *Phys. Rev. E* **2000**, *61*, 475.
(15) Deegan, R. D.; Bakajin, O.; Dupont, T. F.; Huber, G.; Nagel, S. R.; Witten, T. A. *Phys. Rev. E* **2000**, *62*, 756.
(16) Rabani, E.; Reichman, D. R.; Geissler, P. L.; Brus, L. E. *Nature* **2003**, *426*, 271.
(17) Lin, Z. Q.; Granick, S. *J. Am. Chem. Soc.* **2005**, *127*, 2816.
(18) Hong, S. W.; Xu, J.; Xia, J.; Lin, Z. Q.; Qiu, F.; Yang, Y. L. *Chem. Mater.* **2005**, *17*, 6223.
(19) Xu, J.; Xia, J.; Hong, S. W.; Lin, Z. Q.; Qiu, F.; Yang, Y. L. *Phys. Rev. Lett.* **2006**, *96*, 066104.
(20) Hong, S. W.; Giri, S.; Lin, V. S. Y.; Lin, Z. Q. *Chem. Mater.* **2006**, *18*, 5164.
(21) Wang, Z. L.; Song, J. H. *Science* **2006**, *312*, 242.

NL0624061